International Immunopharmacology 71 (2019) 301–312

Contents lists available at ScienceDirect

International Immunopharmacology

journal homepage: www.elsevier.com/locate/intimp

Protective effects of ambroxol in psoriasis like skin inflammation: Exploration of possible mechanisms

Shruthi Sunkari[1], Sowjanya Thatikonda[1], Venkatesh Pooladanda, Veerabhadra Swamy Challa, Chandraiah Godugu*

Department of Regulatory Toxicology, National Institute of Pharmaceutical Education and Research (NIPER), Balanagar, Hyderabad, Telangana 500037, India

ARTICLE INFO

Keywords:
Ambroxol
Lipopolysaccharide
Imiquimod
Oxidative-nitrosative stress
Psoriasis

ABSTRACT

The purpose of this study was to investigate the protective effects of ambroxol in psoriasis-like skin inflammation both *in vitro* and *in vivo* and delineate the molecular mechanism of ambroxol. Our data demonstrated that ambroxol has an imperative role in inhibiting the lipopolysaccharide (LPS) stimulated nitrite levels, total cellular and mitochondrial reactive oxygen species level which was determined by Griess assay, DCFDA, and MitoSOX Red staining, respectively. We found that ambroxol remarkably reduced imiquimod (IMQ) induced epidermal hyperplasia, psoriasis area and severity index (PASI) scoring, splenomegaly, skin, and ear fold thickness. In addition, the histopathological evaluation revealed that ambroxol topical and subcutaneous treatment eloquently reduced psoriasiform lesions including acanthosis. Moreover, with ambroxol intervention, the levels of antioxidants glutathione (GSH), superoxide dismutase (SOD), and IL-10 were found to be increased along with a reduction in nitrite levels in skin tissues. On the other hand, ambroxol treatment significantly reduced imiquimod-induced levels of inflammatory cytokines such as IL-1β, IL-6, IL-17, IL-22, IL-23, TGF-β, and TNF-α. Furthermore, from immunoblotting, we found a decrease in the protein expression of nitrotyrosine, iNOS, NF-κB and MAPKs signaling cascade with a concomitant increase in the expression of Nrf-2 and SOD-1 in RAW 264.7 cells and skin tissues by ambroxol. Similar findings were observed by immunofluorescence in macrophages. Moreover, ambroxol downregulated the ICAM-1 and Ki67 expression observed in skin tissues. Collectively, our results demonstrate that ambroxol may have intriguing therapeutic possibilities in attenuating psoriasis.

1. Introduction

Psoriasis is a chronic autoimmune disease mediated by dysregulated immune responses from macrophages, T-cells and dendritic cells (DC), which results in hyperproliferation of keratinocytes in the epidermis [1,2]. Th17 axis with particular emphasis towards IL-17A, IL-22, and IL-23 cytokines has gathered much of the limelight in the psoriasis pathogenesis [3]. The prevalence rate of psoriasis in western populations is estimated to be around 2–3% and has a chronic relapsing treatment course that persists for the lifetime of an affected individual and places a substantial economic burden [4]. A recent study reported the annual direct and indirect costs of psoriasis are about approximately $112 billion in the U.S.A. [5]. Biologics including infliximab, adalimumab, secukinumab, and ustekinumab have clinically proven efficacy, but their use is associated with a much higher cost compared to the traditional treatment options [6]. Conventional systemic therapies including methotrexate and photo-therapies have proven efficacy and affordability but associated with systemic toxicity on prolong usage. Tacrolimus, acitretin, and cyclosporine-A are other common drugs used in psoriasis with inherent side effects [7]. Topical tacrolimus is prescribed for the treatment of psoriasis with promising efficacy and benefit over calcipotriol [8] but may have the potential to increase the risk of lymphoma and skin cancer [9]. Therefore, psoriasis disease warrants long term affordable, safe, and efficacious therapies to halt the dysregulated signaling preferably in topical route, as psoriasis is the disease of skin the pharmacodynamic effect needed thereof is local.

The growing body of literature suggests that increased reactive oxygen species (ROS) and reactive nitrogen species (RNS) exacerbate the psoriasis pathogenesis. One important line of defence, which could suppress ROS mediated effects are endogenous enzymes, including glutathione peroxidase (GSH), superoxide dismutase (SOD), and catalase (CAT) which counter-regulate the harmful oxidants [2]. Compromised antioxidant defence system further results in lipid peroxidation, DNA modification, and secretion of inflammatory cytokines which

* Corresponding author.
E-mail address: chandra.niperhyd@gov.in (C. Godugu).
[1] Authors contributed equally.

https://doi.org/10.1016/j.intimp.2019.03.035
Received 16 October 2018; Received in revised form 26 February 2019; Accepted 20 March 2019
Available online 29 March 2019

attribute to skin inflammation [2,10]. Nonetheless, the reduction in levels of aberrant RNS and ROS has paramount importance in the therapy of psoriasis.

It has been postulated from previous studies that the signaling pathways including nuclear factor kappa-light-chain-enhancer of activated B cells (NF-κB) and the mitogen-activated protein kinases (MAPKs) are crucial regulatory elements involved in the immune-inflammatory responses implicated in the etiology of psoriasis [11,12]. Activation of NF-κB signaling triggers inflammatory cytokines, also upregulates the inducible Nitric Oxide Synthase (iNOS). Conversely, it has been observed from the previous studies that activity of NF-κB is also activated by ROS [13,14]. Involvement of this signaling cascade in psoriasis has been gaining considerable attention. The MAPKs are among the intracellular signaling pathways, which are principally involved in mediating cell proliferation, differentiation, and inflammation [15]. Four different distinctly regulated groups of MAPK have been identified, these include extracellular signal-regulated kinase 1 and 2 (ERK1/2), c-Jun N-terminal kinase (JNK), p38, and ERK5. Recent findings suggest that there is significant involvement of p38 and ERK1/2 in the lesional psoriatic skin as compared to non-lesional psoriatic skin. Similarly, Takahashi et al. found increased ERK1/2, as well as JNK expression in the nuclei of the inflammatory epidermis [15]. Overall, this complex interplay between the inflammatory signaling mechanisms and oxidative-nitrosative damage could lead to abnormal activation of the innate and adaptive immune system as well as dysfunctional keratinocytes that drive the immune pathological process of psoriasis.

Ambroxol (AMB), an active metabolite of bromhexine, isolated from the plant species *Adhatoda vasica* [16]. AMB is clinically evaluated for the treatment of respiratory diseases associated with viscid or excessive mucus in chronic bronchitis [17]. In addition, AMB is endowed with the capacity to exert anti-inflammatory, antiviral, antibacterial, antifungal, and anti-fibrotic activities, through the overwhelming mechanistic properties including antioxidant potential by scavenging free radicals, reduction in histamine and leukotriene release from human mast cells and leukocytes [18,19]. Moreover, AMB has been reported to reduce pro-inflammatory cytokines and chemokines release from macrophages by inhibiting lipopolysaccharide (LPS)-induced oedema, neutrophil infiltration, exudation, and lung haemorrhage similar to dexamethasone with low adverse reactions and found to be cost-effective [16,20–22]. Additionally, AMB is also reported as glucocerebrosidase enhancer in Gaucher's disease [23,24].

In accordance with the aforementioned intriguing influence of oxidative stress on the immune-mediated inflammation in psoriasis, and the imperative properties of AMB in reducing oxidative damage and inflammation. Here, we have speculated the positive effects of AMB in ameliorating the psoriasis like skin inflammation.

2. Materials and methods

2.1. Chemicals and reagents

Lipopolysaccharide (LPS) from *Escherichia coli*, Ehrlich reagent, 5,5-dithio-bis(2-nitrobenzoic acid) (DTNB), Potassium chloride, Sodium dodecyl sulphate (SDS), Formaldehyde, Tris-HCl, Glycine, 3-(4,5-dimethylthiazol- 2-yl)-2,5-diphenyl tetrazolium bromide (MTT), 2′,7′-dichlorodihydrofluorescein diacetate (DCFDA), Griess reagent, Dimethyl sulfoxide (DMSO), Reduced glutathione (rGSH), and Sodium hydroxide were purchased from Sigma-Aldrich, USA. Enzyme-linked immunosorbent assay (ELISA) kits for IL-1β, IL-6, IL-17A, IL-22, TNF-α, and TGF-β were procured from Thermo Scientific, USA. IL-23 ELISA kit was procured from R&D Systems, USA. AMB was obtained as a gift sample from Hetero Labs Ltd., India. Nitrocellulose membrane and enhanced chemiluminescence (ECL) substrates were purchased from Biorad, USA. Dulbecco's Modified Eagle's medium (DMEM), Roswell Park Memorial Institute medium 1640 (RPMI-1640), Fetal bovine serum (FBS), Trypsin-EDTA and Antibiotics-antimycotics were purchased from Thermo Fisher Scientific, USA. Anti-ICAM1, Anti-nitro tyrosine, anti-Nrf-2, anti-SOD1, anti-Ki67, and β-Actin antibodies were purchased from Santa Cruz Biotechnology, USA. Anti-iNOS antibody was obtained from Sigma-Aldrich, USA. Anti-p-NF-κB (p-p65), anti-NF-κB (p65), anti-p-p38-MAPK, anti-p38-MAPK, anti-p-JNK, anti-JNK, anti IL-10 antibodies were purchased from Cell Signaling Technologies, USA. All secondary anti-rabbit and anti-mouse antibodies were procured from Santa Cruz Biotechnology, USA. All other chemicals were of analytical grade and obtained commercially.

2.2. Cell culture

Mouse macrophages (RAW 264.7) were obtained from National Centre for Cell Science (NCCS), Pune, India and human keratinocytes (HaCaT) cell line was a kind gift sample from Dr. Munia Ganguli, Institute of Genomics & Integrative Biology (IGIB), New Delhi, India. Both the cell lines were grown in DMEM and RPMI-1640 media, respectively supplemented with 10% FBS and stabilized with 1% antibiotic-antimycotic solution in an incubator with 5% CO_2 and 98% relative humidity at 37 °C in the incubator. When the cells reached 80–90% of confluence, cells were treated with 0.25% trypsin/1 mM EDTA solution for further passage. Stock solutions of AMB (10 mM) were dissolved in DMSO and stored at −80 °C, and diluted in fresh medium immediately before use.

2.3. Determination of cell viability by MTT assay

The MTT assay is a colorimetric assay for assessing cell metabolic activity. In this assay, HaCaT and RAW 264.7 cells were seeded in a 96-well plate and allowed to adhere for 24 h. Then the cells were treated with AMB at two-fold serial dilution and incubated for 48 h. Then the medium was completely removed and replaced with MTT dye (0.5 mg/ml) and incubated for 4 h, then the insoluble formazan crystals formed were solubilized in DMSO and the absorbance was taken at 570 nm in the multidetection plate reader (Spectramax M4, Molecular Devices, USA) [25].

2.4. Measurement of nitrite levels by Griess assay

Griess assay is used for the determination of nitrite levels as nitrite represents the final product of nitric oxide (NO) oxidation pathway was measured analytically from cell culture supernatant as an indicator of NO production based on the Griess reaction. Briefly, RAW 264.7 cells were cultured and treated with various concentrations of AMB at 0.1, 0.5, 1, and 2.5 μM for 24 h followed by LPS stimulation (1 μg/ml) for 24 h. Later, from each group, 100 μl of cell supernatants were collected and mixed with 100 μl of Griess reagent (1% sulfanilamide, 0.1% naphthyl ethylenediamine, and 2.5% H_3PO_4) and incubated at room temperature for 10 min, and then the absorbance was measured at 540 nm using a multimode plate reader [26].

2.5. ROS detection in RAW 264.7 and HaCaT cells

Total cellular and mitochondrial ROS levels were examined using DCFDA and MitoSOX™ Red staining, respectively. To measure the ROS levels, RAW 264.7 and HaCaT cells were seeded in 6-well plates and treated with AMB for 24 h, and then the ROS was induced by LPS (1 μg/ml) for 30 min. Later, DCFDA (10 μM) or MitoSOX™ Red (5 μM) was added and incubated for 20 min at 37 °C in the dark, respectively. Then, the cells were trypsinized and subjected to flow cytometry (BD Accuri C6 flow cytometer, USA) and relative geo-mean was measured. For visualization, treated cells were captured by Nikon Eclipse inverted microscope, Japan at x200 magnification immediately following dye exposure [26] with excitation/emission 498/530 nm for DCFDA and 510/580 nm for MitoSOX Red, respectively.

2.6. Immunofluorescence (IF)

RAW 264.7 cells were seeded in cell imaging chambers (Eppendorf, Germany), and treated with AMB (1 μM) for 24 h. followed by LPS induction for 12 h. Then the cells were fixed with 4% paraformaldehyde for 5 min at room temperature. After fixation, cells were rinsed with immuno wash buffer three times for 5 min each and permeabilized with 0.1% Triton-X-100. Cells were blocked with 3% BSA and incubated with primary antibody overnight at 4 °C. After washings, relevant fluorescent dye-conjugated secondary antibodies were added and incubated for 1 h at room temperature. The coverslips were mounted onto chamber glass slides with Fluor shield™ histology mounting medium with DAPI nuclear stain (Sigma-Aldrich, USA). Images of the stained slides were captured by Leica TCS SP8 Laser Scanning Spectral Confocal Microscope. The primary antibodies were used as follows: rabbit NF-κβ p65, Nrf-2 (Cell Signaling Technology, USA; 1:200) and mouse anti-SOD1 as well as nitrotyrosine (Santa Cruz Biotechnology, USA; 1:200). Anti-rabbit and anti-mouse antibodies were conjugated to FITC and rhodamine (Cell Signaling Technologies, USA) were used as secondary antibodies at 1:200 dilution.

2.7. Ethical statement

The study was carried out in BALB/c male mice (weight 25–30 g) of age range 6–8 weeks were purchased from Palamur Biosciences, India. Animals were housed (3 animals per cage) under specific pathogen-free conditions with a 12 h light/dark cycle. All animals were acclimatized at least one week prior to initiating the experiment. All procedures of the study were approved by the Institutional Animal Ethics Committee (Approval No: NIP/01/2018/RT/274), NIPER-Hyderabad, India. All the experiments were conducted in accordance with the Committee for the Purpose of Control and Supervision of Experiments on Animals (CPCSEA) guidelines, the government of India.

2.8. IMQ induced psoriatic plaque model

IMQ model for psoriasis-like skin inflammation in BALB/c mice was developed as described by Van Der Fits et al. [27]. The mice were divided into six groups with $n = 5$ per group. Marketed Imiquimod cream (Imiquad cream, 5% w/w, Glenmark Pharmaceuticals Ltd., India) was applied topically on to the shaven back dorsal region of the skin and left ear of BALB/c mice at a dose of 62.5 mg/day per 5 cm^2 surface area for all groups except normal control for 6 days. IMQ control group received no AMB; the low dose (AL) and high dose (AH) groups received 10 and 30 mg/kg of AMB topically. The subcutaneous group (ASC) received 2 mg/kg injection and the standard tacrolimus (TAC) group received 20 mg/kg per mice topically. Treatment was initiated from day three of IMQ administration, once a day continued till 6 days. The psoriasis severity was monitored and Psoriasis Area Severity Index (PASI) was graded alternate day [28], Skin fold and ear fold thickness was measured by Vernier callipers (M & W precision tools, India). After seven days mice were sacrificed and skin samples were collected and stored at −80 °C.

2.9. Spleen to body weight index

Spleen images were captured using a digital camera and observed for spleen morphology. Animal body weights were recorded until the termination of the study and after sacrifice spleens were collected, cleaned and weighed. The spleen weights were normalized with body weight to obtain organ index (Spleen weight/Bodyweight) and results were expressed in g/g.

2.10. Biochemical parameters in skin tissue samples

Ellman's method was used to measure the glutathione content in skin tissue supernatants. Skin tissues were homogenized in PBS on ice by using homogenizer and then centrifuged at 12,000 rpm at 4 °C for 10 min. The supernatant of homogenized skin tissue samples containing GSH buffer was collected and Ellman's reagent [5,5′-dithiobis-2-nitro benzoic acid (DTNB) solution] was added to the supernatants. The protein concentration in the supernatants was determined by the Bradford method using bovine serum albumin (BSA) as a standard. After 5 min incubation in dark condition, absorbance was measured at 412 nm. Values obtained were compared with a series of rGSH standards. Results were expressed as μM/mg of protein.

2.11. Estimation of LPS and IMQ induced nitrite levels

As discussed earlier, the nitrite levels were estimated using Griess reagent. An equal volume of Griess reagent and supernatants of homogenized skin tissue samples were mixed and incubated in dark for 10 min and absorbance was measured at 548 nm. Nitrite levels were expressed as μM/mg of skin protein with sodium nitrite as standard.

2.12. Estimation of superoxide dismutase levels

SOD activity was measured as per the method described by Umasuthan et al. [29]. SOD was estimated in skin tissue homogenates based on the generation of superoxide radicals produced by xanthine and xanthine oxidase that form a red formazan dye. Briefly, the assay was performed triplicate in a 96 well plate. Each well contained 160 μl of 0.1 M glycine-NaOH buffer (pH 9), EDTA (3 mM), BSA (0.15%), NBT (0.75 mM), 6.75 μl of each xanthine (3 mM), and 20 μl sample. After equilibration at 20 °C for 10 min, the reaction was initiated by adding 6 mU of xanthine oxidase and incubated further at 20 °C for 20 min. After incubation reaction was terminated by addition of 6.75 μl of 6 mM $CuCl_2$ and absorbance was measured at 560 nm by the multimode plate reader.

2.13. Hematoxylin and eosin (H&E) staining

The dorsal region of the skin from all mice groups was collected and fixed in 10% formalin solution and embedded in paraffin. Tissue processing was done as per the standard procedure [30].The paraffin-embedded sections were then cut to a thickness of 5 μm and stained with H & E for histological evaluation.

2.14. Enzyme-linked immunosorbent assay (ELISA) for cytokines evaluation

Topical administration of IMQ results in proliferation of keratinocytes *via* elevation of multiple inflammatory cytokines [31]. The levels of proinflammatory cytokines were measured by ELISA assay as reported earlier [32]. Briefly, the skin tissues were homogenized in Tris-HCl buffer with protease and phosphatase inhibitors. After that skin homogenates were centrifuged (12,000 rpm, 4 °C, for 10 min) and the protein content was estimated in collected supernatants by Bradford's reagent. After estimating protein concentration, as per the manufacturer's instructions polystyrene 96 well plates were coated with IL-1β, IL-6, IL-17A, IL-22, IL-23, TGF-β, and TNF-α separately with capture antibodies (100 μl/well diluted with coating buffer) and incubated overnight at 4 °C. Next day, wells were aspirated with washing buffer and blocked with 200 μl of blocking buffer for 1 h. Following the aspiration, wells were incubated with 100 μl of sample overnight. After incubation detection antibody was added and kept for 1 h at room temperature. The plates were incubated with 100 μl/well of Avidin-HRP solution for 30 min and then washed. After this step, 100 μl/well trimethylbenzidine solution was added and incubated for 15 min and then the reaction was stopped using 1 M H_3PO_4. The absorbance was measured at 450 and 570 nm wavelength and the difference was calculated. The results were expressed in pg/mg of protein.

2.15. Western blot analysis

Immunoblot analysis was performed to delineate the mechanism of AMB in modulating oxidative-nitrosative stress and associated signaling pathways. Whole cell protein was extracted from cells and skin tissue lysates as per the previously reported method with slight modifications [33]. Briefly, cultured cells and skin tissues were incubated with pre-cooled lysis buffer containing protease inhibitors and kept on ice bath with 10 s vortexing for every 10 min interval for 3 times, followed by centrifugation at 12000 rpm and 4 °C for 10 min and the supernatant was collected and protein content was estimated by BCA colorimetric assay kit (Sigma-Aldrich, USA). Then, samples were subjected to SDS-PAGE and were electrotransferred to nitrocellulose membrane and blots were blocked with 3% BSA at room temperature for 1 h and probed with primary and secondary antibodies. After washing three times (for 5 min each) in Tris-buffered saline with tween 20 (TBS-T), pH 7.5, enhanced chemiluminescence (ECL) solution was added and exposed to Chemdoc imaging system (Vilber Fx, France). β-Actin was used as a housekeeping protein for normalization of different proteins expression. Band intensities of blots were quantified using Image J software, NIH, USA.

2.16. Immunohistochemistry (IHC) and immunofluorescence (IF)

5 μm skin sections were deparaffinized, rehydrated and subjected to antigen unmasking with proteinase K 15 min. Non-specific binding from the sections were eliminated using 3% BSA blocking solution. Further steps were carried out as per the method reported by Venkatesh et al. [34]. Then the sections were incubated with anti-ICAM1 (1:100 dilution) primary antibody overnight at 4 °C. The further procedure was performed with the PolyExcel HRP/DAB Detection System kit (Pathn-Situ Biotechnologies, USA) and followed the manufacturer instructions, the immune reactions were visualized by adding the DAB (3,3′-diaminobenzidine tetrachloride) and the sections were counterstained with hematoxylin for IHC. For IF analysis after incubation with Ki67 (1:100 dilution) primary antibody at 4 °C overnight, sections were washed thrice using immuno wash buffer followed by the addition of Fluorescein isothiocyanate (FITC) anti-rabbit antibody (1:200 dilution) for 1 h at room temperature, washed and mounted and were visualized using a confocal microscope.

2.17. Statistical analysis

Results were expressed as the mean ± standard deviation (SD) and n refers to the number of sample replicates. One-way ANOVA was applied with the Bonferroni *post hoc* test for statistical analysis. Prism software (version 6.01; GraphPad, USA) was used to analyze the data and $P < 0.05$ was considered to be statistically significant.

3. Results

3.1. AMB inhibits LPS-induced nitrite levels in RAW 264.7 cells

Anti-inflammatory and anti-oxidative properties of AMB were evaluated in psoriasis like inflammatory disease both *in vitro* and *in vivo*. Initially, MTT assay was used to assess the effect of AMB (Fig. 1A) on the viability of epidermal keratinocytes and murine macrophages. The results showed that AMB had not shown the significant reduction in cell viability up to 2.5 μM on murine macrophages (Fig. 1C) whereas, in keratinocytes, AMB was found to be safe up to 5 μM with less significant cytotoxicity (Fig. 1B). Maximum safe concentrations 0.1, 0.5, 1 and 2.5 μM of AMB were treated in RAW 264.7 cultured cells to analyze the nitrite levels induced by LPS in the culture medium as an index of NO synthesis. As shown in Fig. 1D, increased nitrite production was observed after LPS (1 μg/ml) stimulation as compared to unstimulated macrophages, it was also evident that there was a decrease in the nitrite levels with AMB treatment suggesting the inhibitory effect on nitric oxide production.

3.2. AMB reduces LPS induced cellular and mitochondrial ROS levels in HaCaT and RAW 264.7cells

LPS stimulation induced total cellular oxidant levels and mitochondrial superoxide generation, and the role of AMB against ROS generation was measured in keratinocytes and macrophages. Consistent with the previous reports [35], an increase in cellular ROS production due to oxidative conversion of non-fluorescent 2′,7′-dichlorodihydrofluorescein (H2DCF) into fluorescent 2′,7′-dichlorofluorescein (DCF) (Fig. 2A & C) and oxidation of MitoSOX Red reagent by superoxides in mitochondria was observed in both cells (Fig. 2B & D) in comparison to control cells. For quantitative measurement to assess cellular and mitochondrial redox status, flow cytometry analysis was performed (Fig. 2E & F). It was found that AMB significantly attenuated LPS induced cellular ROS generation and mitochondrial superoxide levels suggesting the effective radical scavenging effects of AMB in a concentration-dependant manner in both the assays.

3.3. AMB inhibits LPS driven oxidative-nitrosative stress and inflammation in cultured macrophages

Oxidative-nitrosative stress has been linked to alteration of inflammatory signaling cascade including MAPKs and NF-κB. Therefore, to delineate the possible involvement of AMB treatment in the modulation of these signaling pathways, AMB mechanism was examined by immunoblotting. Cells were pre-treated with AMB for 24 h followed by LPS stimulation and further incubated for 24 h. It was observed that AMB treatment dose-dependently attenuated the expression of nitrotyrosine and iNOS, and concomitantly increased the expression of anti-oxidant regulators Nrf-2 and SOD1 (Fig. 3A–E). The immunoblotting results indicated that exposure of RAW 264.7 to LPS stimulation (1 μg/ml), markedly promoted the phosphorylation of three MAPKs including JNK, p38 MAPK and ERK1/2, on the other side increased phosphorylation of NF-κB was observed after 30 min of post LPS exposure (Fig. 3F–J). AMB pre-treatment in macrophages with 0.5, 1, and 2.5 μM for 24 h followed by 30 min LPS challenge significantly abrogated the inflammatory response by inactivating the MAPK and NF-κB signaling pathways.

To further confirm the immunoblotting findings, the confocal analysis was performed to investigate SOD1, NF-κB, and Nrf-2 and nitrotyrosine protein expression, it is clearly evident from the results (Fig. 4A & B) that AMB treatment at 1 μM concentration profoundly decreased the expression of NF-κB, nitrotyrosine with increased SOD1 and Nrf-2 expression.

3.4. AMB treatment attenuates signs and symptoms of IMQ-induced psoriasis-like skin inflammation

To assess the effect of AMB on IMQ induced psoriasis, IMQ cream was applied on the shaved back skin of mice for six consecutive days as described previously, showed marked phenotypic changes (scaling and erythema) as observed in Fig. 5A, where the AMB topical administration in BALB/c mice at 10 and 30 mg/kg, as well as SC administered at 2 mg/kg dose along with standard TAC, elicited a remarkable decrease in the phenotypic changes and severity index scoring induced with IMQ application on the skin (Fig. 5C–E). As shown in Fig. 5G & H, the skin fold and ear thicknesses were apparent on day 2 and gradually increased throughout the disease induction period, the thickness was measured every alternate day and continued throughout the experimental period. AMB on topical application significantly reduced the IMQ induced epidermal hyperplasia, with a moderate reduction in SC route. Consistent with the previous reports, IMQ on the topical application for 6 consecutive days induced enlargement of spleen through

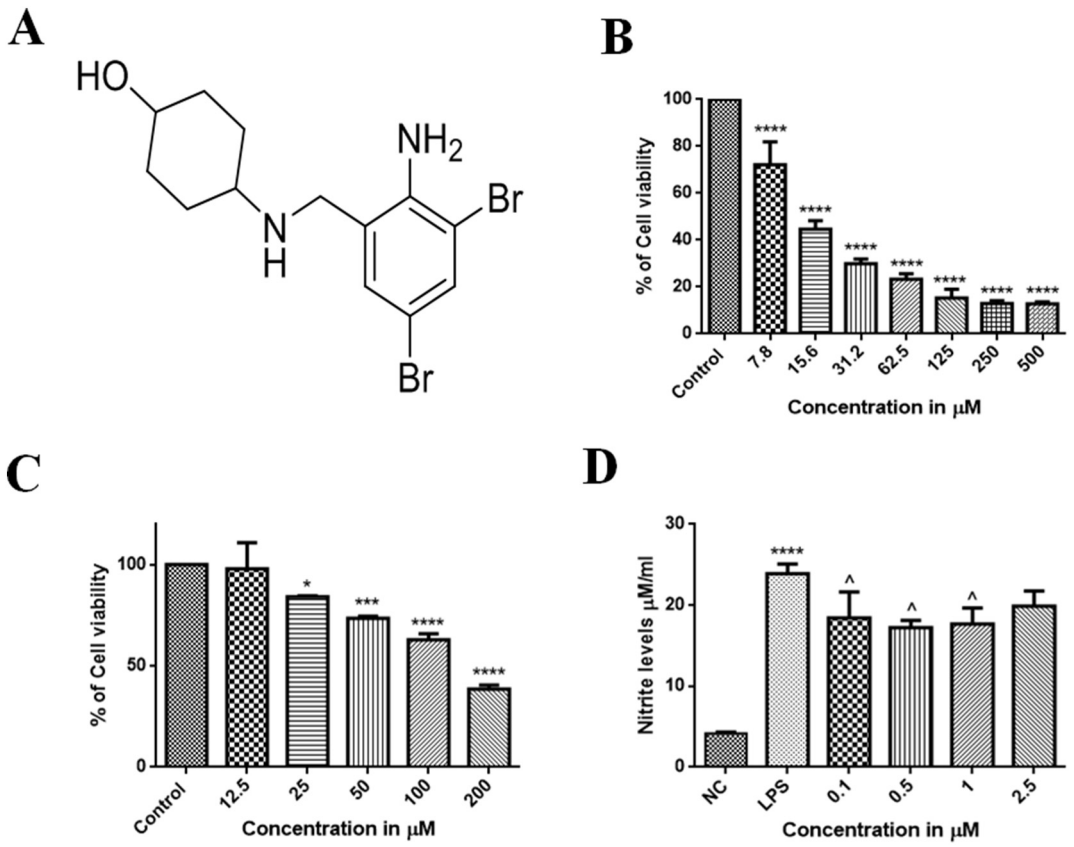

Fig. 1. Effect of Ambroxol (AMB) on cell viability and cellular nitrite levels. (A) Chemical structure of AMB. MTT assay was performed with two-fold serial dilution at various concentrations ranging from 7.8 to 500 μM to determine the percentage cell viability of AMB treatment after 48 h incubation in (B) HaCaT and (C) RAW 264.7, respectively. (D) Griess assay was used to determine the cellular nitrite levels with LPS stimulation and AMB intervention in RAW 264.7 cell culture supernatant.

systemic effects [27]. As shown in Fig. 5B, the spleens of the AMB treated groups in either route were found to be smaller. We further calculated the spleen weight index as the ratio of spleen weight to body weight of the animal. It is evidenced by the results that the spleen index of IMQ group was significantly higher than the control group (Fig. 5F). The results from the spleen index in both routes of AMB treatment resulted in the reduction in size significantly which reflect the systemic therapeutic effect.

3.5. AMB intervention reduced activated skin inflammatory cytokine signaling cascade induced by IMQ and exhibits anti-nitrosative, anti-oxidant, and anti-inflammatory effects

In this study, GSH, SOD, and nitrite levels in the skin were measured in all the groups as per the protocols described in methods. As shown in (Fig. 6A–C), IMQ group showed lower levels of GSH, and SOD, but a higher level of nitrite production compared to control mice. However, upon treatments with AMB at 10 and 30 mg/kg topically and 2 mg/kg in SC routes, the anti-oxidant markers GSH and SOD were elevated significantly (Fig. 6A & B) compared to IMQ control group. Furthermore, AMB treatment reduced skin tissue nitrite levels compared with IMQ group in topical high dose (Fig. 6C) and in SC route moderate reduction was observed. AMB topical at 10 and 30 mg/kg effectively counter-regulated enhanced oxidative/nitrosative stress. T helper Th1 and Th 17 cells mediate persistent inflammation in psoriasis pathogenesis, where, Th1 (TNF-α, IFNγ, and IL-2) and Th17 (IL-17A, IL-17F, IL-22, IL-26, and TNF-α) cytokines levels are up-regulated in the serum of psoriasis patients [36]. Here, IMQ application upregulated the cytokines including IL-1β, IL-6, IL-17A, TGF-β, TNF-α IL-22, and IL-23 significantly (Fig. 6D–J) in comparison with control animals analyzed by ELISA. Interestingly, AMB treatment topically at 10 and 30 mg/kg, dose-dependently attenuated the elevated cytokine levels compared with IMQ group animals. Based on the *in vitro* results, it is intriguing to speculate the role of AMB in IMQ induced psoriasis. To establish anti-psoriatic activity of AMB *in vivo*, we investigated the expression of various proteins involved in nitrosative-oxidative stress and ROS regulated signaling pathways including nitrotyrosine, iNOS, Nrf2, SOD-1, NF-κB (p65), SAPK/JNK, p44/42, p38 MAPK, and the cytokine IL-10 (Fig. 6K–T). AMB intervention led to a significant decrease in the nitrosative-oxidative stress by attenuating ROS and RNS regulated proteins expression while concomitantly increased the expression of anti-inflammatory cytokine IL-10.

3.6. AMB treatment improved the skin epidermal architecture and reduced the expression of adhesion molecule and proliferation marker

The results from histological skin staining showed that IMQ application resulted in signs and symptoms of psoriasis-like skin inflammation including epidermal hyperplasia and acanthosis in mice (Fig. 7A). It was observed from the results, AMB treatment topically at 10 mg/kg (AL), and 30 mg/kg (AH) remarkably attenuated the psoriasiform lesions in comparison to the standard tacrolimus, hence, the protective effect was observed, whereas mild to moderate change was observed with SC route (ASC). To further investigate the effect of AMB treatment, we have analyzed the expression of adhesion and proliferation markers where AMB intervention significantly reduced the expression of both ICAM1 (Fig. 7B) and Ki-67 (Fig. 7C).

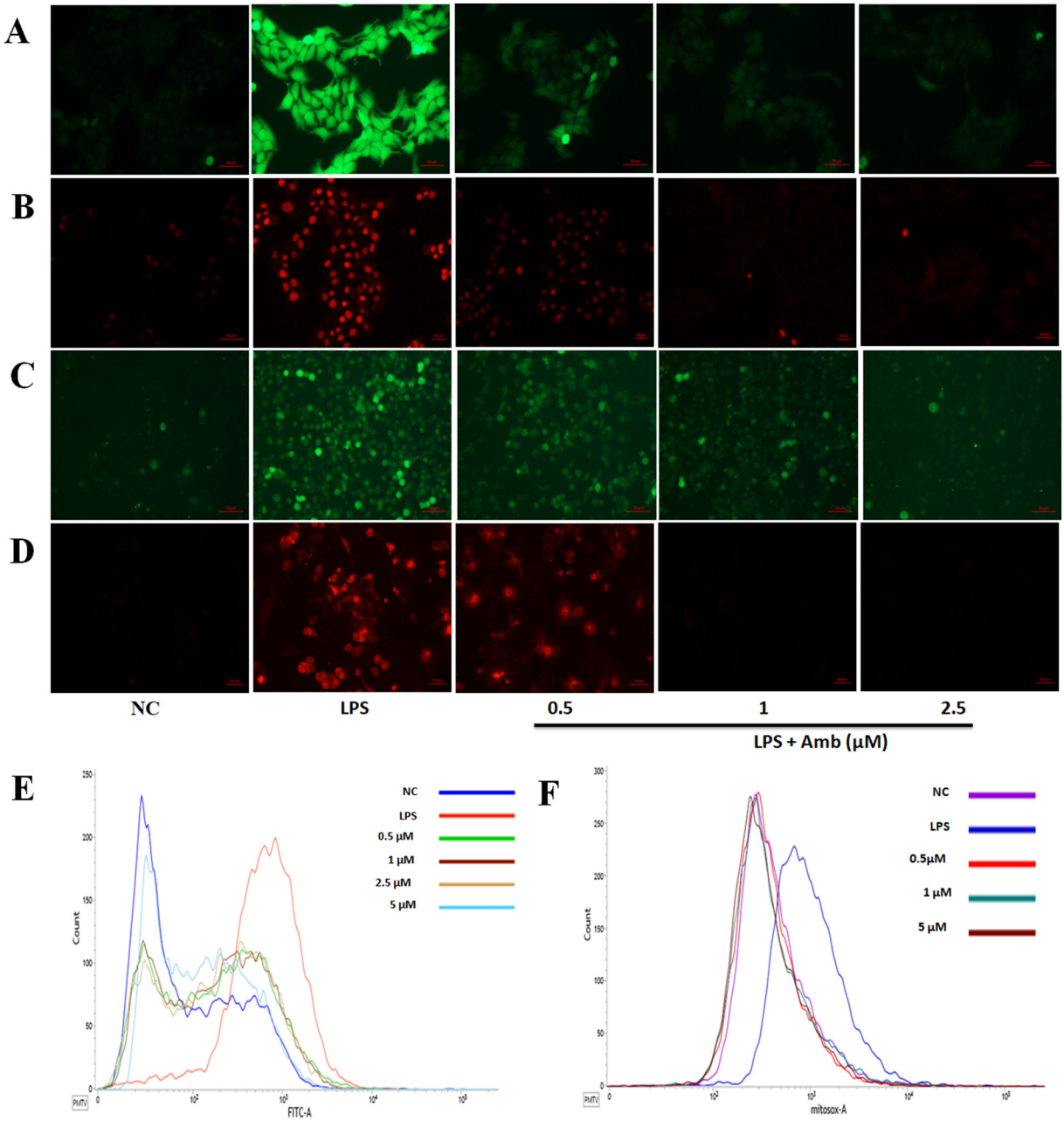

Fig. 2. Effect of AMB on LPS induced total cellular and mitochondrial reactive oxygen species (ROS) levels. DCFDA and MitoSOX Red staining were performed in HaCaT and RAW 264.7 cells by pre-treatment with AMB (0.5 to 5 μM concentrations) for 24 h. Later, cells were stimulated with LPS (1 μg/ml) and incubated for 30 min. (A) The total cellular ROS was examined in HaCaT cells by a fluorescence microscope after DCFDA staining and (B) mitochondrial ROS was detected by MitoSOX Red staining. (C) Intracellular ROS by DCFDA and (D) mitochondrial ROS levels by MitoSOX Red were measured in RAW 264.7 cells by capturing fluorescent images at ×200 magnification (scale bar: 50 μm) and further cells were subjected to flow cytometric analysis for quantitative determination of fluorescence intensity of (E) DCFDA and (F) MitoSOX Red staining.

4. Discussion

Ambroxol, a metabolite of bromhexine, which was approved by US FDA has been established for decades for the treatment of acute and chronic respiratory diseases and has been found to exert an excellent anti-inflammatory and antioxidant activities [37] with high margin of safety in rats (oral route) and humans (oral and I.V. routes) [38,39]. Psoriasis is a multi-factorial disease manifested by oxidative stress, keratinocyte hyperproliferation, persistent inflammation, and abnormal differentiation in the epidermis as the hallmarks of psoriasis [40]. In a complex interplay between the immune system driven by pathogenic T cells and dendritic cells, which migrate to the skin and secrete pro-inflammatory cytokines, including IL-1 β, IL-6, IL-17A, IL-17F, IL-22, IL-23, TNF-α, and TGF-β, which further amplifies psoriatic inflammation, thus lead to uncontrolled keratinocyte hyperproliferation [31,41]. Under normal physiological conditions, ROS is produced and then eliminated by the ROS scavenging system thus maintain cellular redox balance. But, aberrant ROS and RNS species generation has been shown to exert deleterious effects in psoriasis, which feeds a continuous self-perpetuating cycle in mediating inflammation through the highly interconnected cluster. The NO production is catalyzed by a family of enzymes called nitric oxide synthases (NOSs), inducible NOS (iNOS) can be expressed in response to LPS, cytokines and H_2O_2 production [42] and form nitric oxide radicals or $ONOO^-$ in the host cells [43].

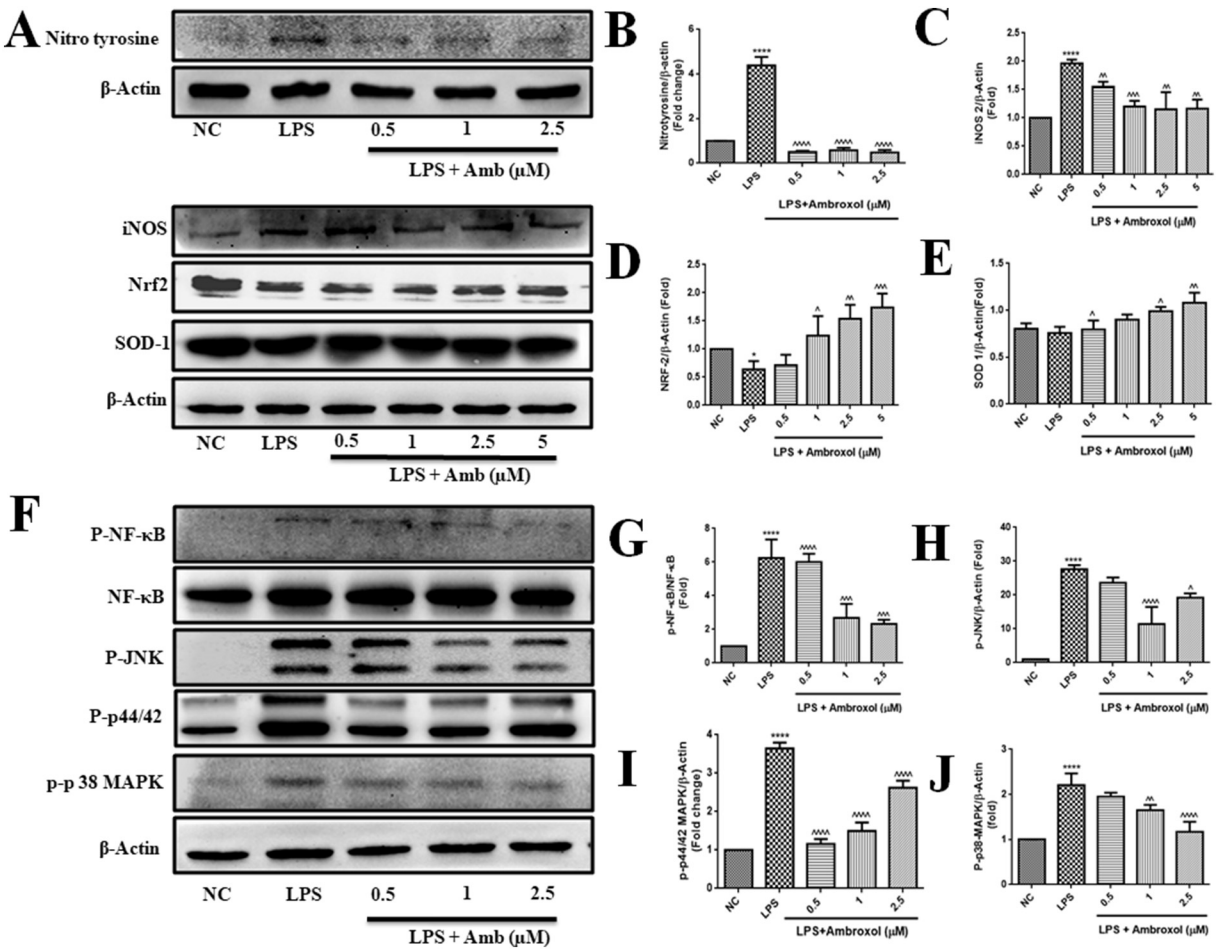

Fig. 3. Effect of AMB on the protein expression of inflammatory stimulus LPS mediated oxidative stress-associated proteins in RAW 264.7 cells. (A) AMB counterbalanced the LPS induced ROS and RNS generation by modulating oxidative and nitrosative stress regulators protein expression where AMB was pretreated for 24 h with and without 1 μg/ml LPS and further incubated for 24 h. The expression of (B) nitrotyrosine, (C) iNOS, (D) Nrf2, (E) SOD1 was studied and quantified by ImageJ, NIH software. ROS regulated redox-associated signaling pathways proteins expression were evaluated by western blotting in RAW 264.7 cells where AMB was pretreated with indicated concentrations for 24 h and was then stimulated with LPS (1 μg/ml) for 30 min (B) and the proteins expression of (G) p-NF-κB, (H) p-JNK, (I) p-p44/42, and (J) p-p38 MAPK were quantitatively determined by ImageJ densitometric analysis.

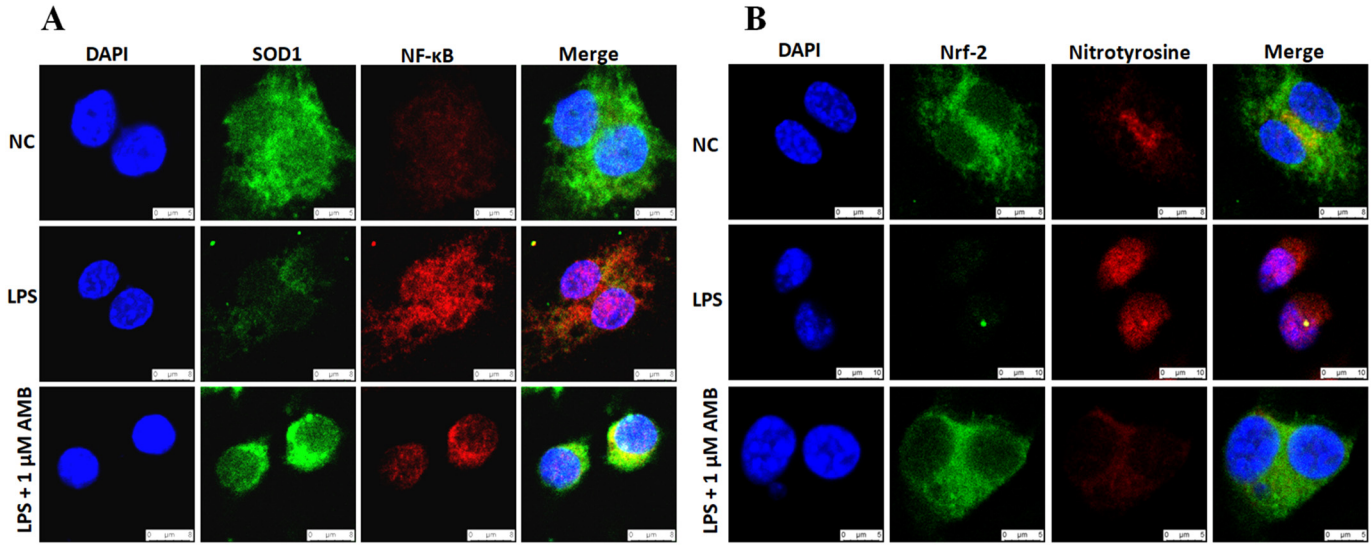

Fig. 4. Effect of AMB on SOD1, NF-κB, Nrf-2 and nitrotyrosine protein expression. Exponentially growing RAW 264.7 were seeded in confocal chambers after adherence, cells were pretreated with AMB (1 μM) and cells were incubated for 24 h and then stimulated with LPS (1 μg/ml). After 12 h, cells were fixed, permeabilized and subjected to IF analysis to observe the expression of (A) SOD1 (green-FITC) and NF-κB (Red-rhodamine) as well as (B) Nrf-2 (green-FITC) and nitrotyrosine (Red-rhodamine) by confocal microscopy. The nucleus was visualized blue due to DAPI (blue). The overlay of two proteins and nuclei were shown as a merged image. (For interpretation of the references to color in this figure legend, the reader is referred to the web version of this article.)

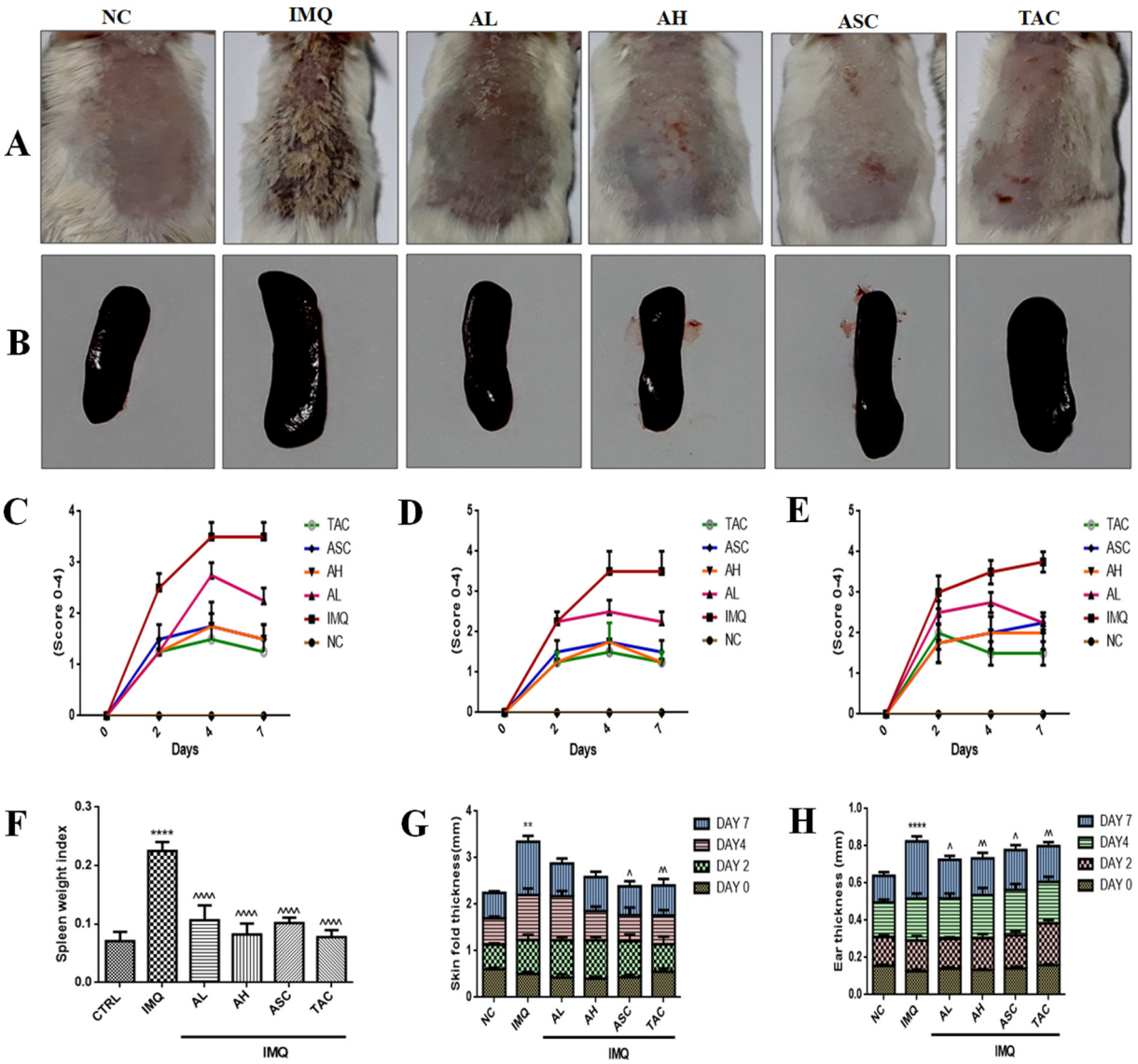

Fig. 5. Effect of AMB on the IMQ-induced psoriasiform severity in BALB/c mice skin resembling human psoriasis. (A) AMB on topical (AL-10 mg/kg; AH-30 mg/kg) and subcutaneous (ASC-2 mg/kg) administration along with the standard (TAC 20 mg/kg) significantly alleviated the phenotypic psoriatic changes on mouse skin after 6 days. (B) AMB treatment significantly reduced the weight and size of the spleen induced by IMQ. PASI scoring of mice on the basis of redness, scaling and thickness that ranges from 0 to 4 (0-none, 1-slight; 2-moderate, 3-marked, and 4-very marked) was recorded on day 0, 2, 4, and 7 and the cumulative scores of (C) redness (erythema), (D) scaling (appearance of skin lesions) and (E) thickness (hardening of the skin), which was elevated on day 2, 4, and 6 days with IMQ application, and reduced effectively by AMB in both topical and SC routes in comparison with TAC as shown for each group. (F) Spleen mass was calculated by body mass index (spleen weight alone/total body weight) in topical and SC routes of AMB administration in comparison to IMQ control. (G) Skin thickness and (H) ear thickness were measured from day 0, 2, 4, and 7 of IMQ administration by Vernier callipers.

Previous studies indicated that elevated levels (> 10-fold iNOS levels) has been found in psoriasis lesions and forms the end product nitric oxide. In an attempt to mimic the oxidative-nitrosative stress, macrophages were stimulated with LPS, which is well-documented in previous reports by several researchers [44,45]. Initially, we performed the Griess assay to measure nitrite levels which is a stable end-product of NO, consistent with the study performed by Michelle et al. [46], where we found a statistically significant increase in the nitrite levels in cell culture supernatants. Additionally, LPS stimulation elevated total cellular and mitochondrial ROS generation in murine macrophages which were analyzed by DCFDA and MitoSOX Red staining. AMB intervention clearly reduced the nitrite levels, total cellular and mitochondrial ROS generation. On the other side, it has been reported that the compromised function of total antioxidant status may worsen the disease progression. One important line of the defence system is tripeptide glutathione and antioxidant enzyme, superoxide dismutase (SOD), and the levels were found to be reduced with IMQ application [47]. A substantial number of studies indicated the potential use of various compounds with antioxidant properties by elevating the levels SOD, CAT, and GSH and scavenging ROS are effective in ameliorating the psoriasis symptoms [26,40]. We also found a positive correlation in immunoblot analysis with the reduced Nrf-2 and SOD-1 protein expression and simultaneously increased expression of nitrotyrosine and iNOS both in LPS induction and IMQ application, and the expression of Nrf-2 and SOD-1 was significantly up regulated by AMB with in a dose dependent manner thus substantiating RNS mediated deleterious effects. On the other hand, AMB exerted the pharmacological potential by ameliorating the expression of RNS regulators such as nitrotyrosine and iNOS in both LPS and IMQ induction models.

We next intended to unravel the mechanisms underlying the anti-psoriasis effect by AMB and to further understand the molecular mechanism, we extended our findings towards TLR-4 and TLR-7 triggered

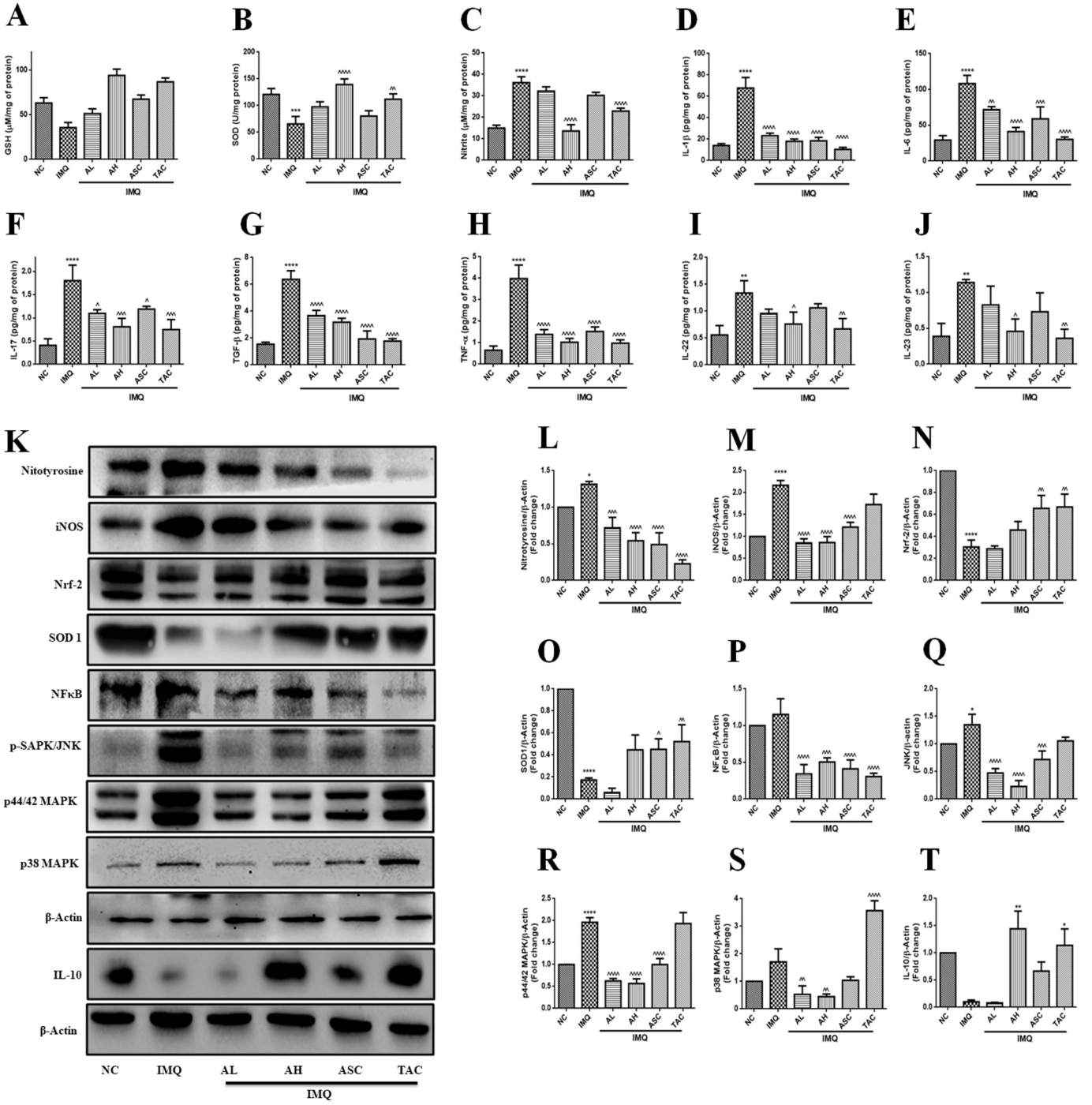

Fig. 6. Effect of AMB on skin tissue oxidative stress markers and pro-inflammatory cytokines. AMB upon topical and SC administration elevated the (A) GSH and (B) SOD levels, while decrease in the skin tissue (C) nitrite (NO_2^-) levels was observed. AMB treatment ameliorated T cell mediated inflammatory cytokines production including (D) IL-1β, (E) IL-6, (F)IL-17A, (G), TGF-β, (H) TNF-α, (I) IL-22, and (J) IL-23 induced by IMQ application the cytokine levels were evaluated by ELISA and compared with the standard TAC cream (K) Immunoblotting showing the effect of AMB on imiquimod induced nitrosative and oxidative stress markers and the inflammatory signaling cascade in the skin tissues the proteins were normalized with β-Actin. The expression of (L) nitrotyrosine, (M) iNOS, (N) Nrf2, and (O) SOD-1 as well as ROS regulated redox-associated signaling pathways (P) NF-κB, (Q) SAPK/JNK, (R) p44/42, (S) p38, and (T) IL-10 were determined and quantified by ImageJ.

crucial signaling cascades, MAPKs (p38, ERK, and JNK) signaling and a protein transcription factor NF-κB, which intricates the inflammatory milieu that contributes to epidermal hyperproliferation and the psoriatic pathogenesis [11,48–50]. Hence, the anti-psoriatic therapies targeting the aberrant signaling while limiting unintended effects are needed. In the present study, our *in vitro* data, coupled with the *in vivo* immunoblotting it was observed that AMB significantly attenuated LPS and IMQ mediated TLR-4 and TLR-7 induced activation of the aforementioned signaling cascade. Nevertheless, in agreement with others, JNK signaling as well as NF-κB plays a vital role in the LPS-stimulated NO production through iNOS expression and also involve in ROS generation [50]. The precise mechanism underpinning this observation was of great interest. Hence, in order to further confirm these effects IF was performed on RAW 264.7 cells, where it was clearly observed that AMB

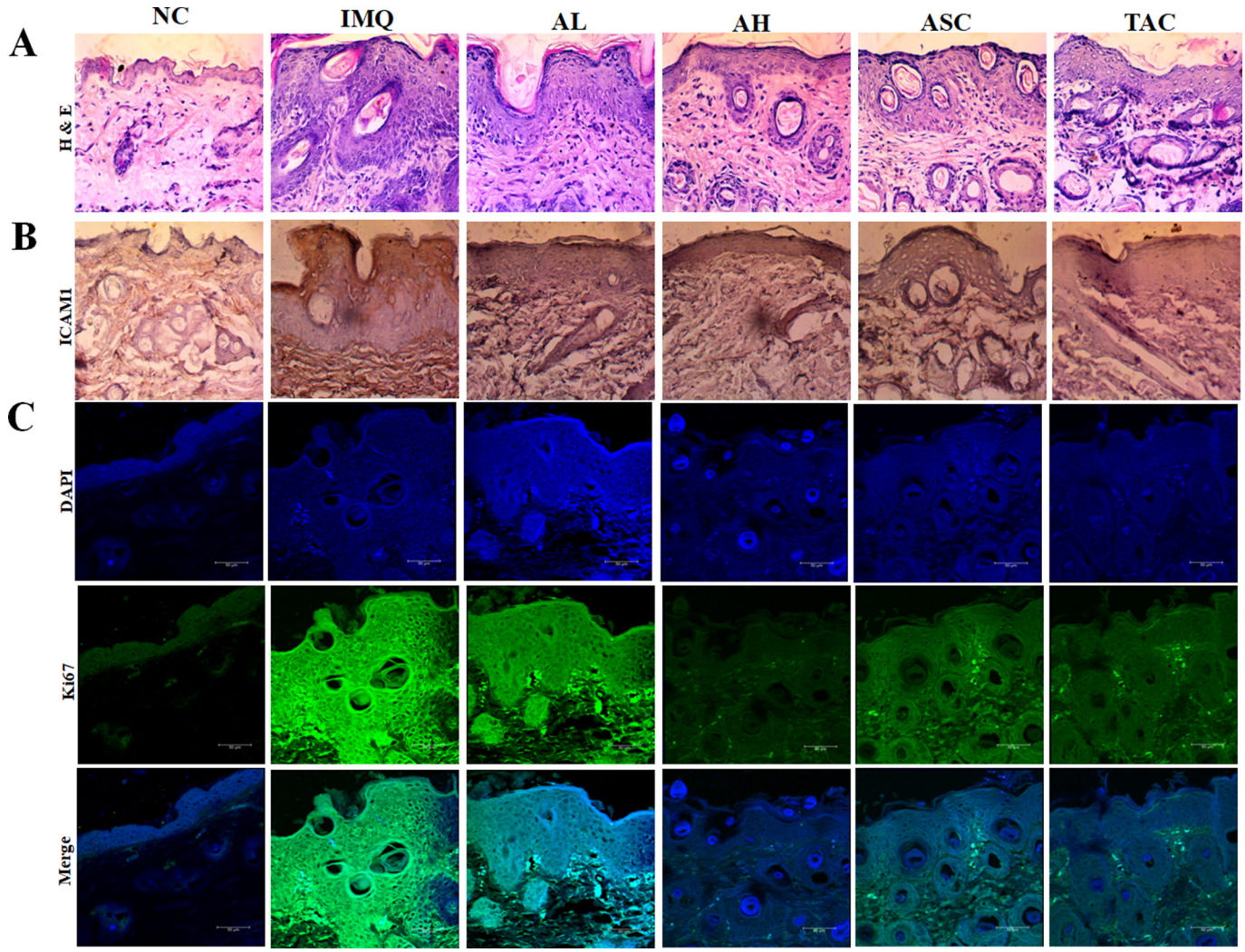

Fig. 7. Effect of AMB on pathological consequences. Skin tissue sections from different groups were fixed in 10% formalin and sectioned at 5 μm and stained with (A) Hematoxylin & Eosin, where IMQ induced phenotypic skin changes resembling human psoriasis including thickened epidermis and topical and sc application of AMB significantly alleviated the psoriasis severity including inhibition of epidermal hyperproliferation in BALB/c mice. The IHC and IF analysis was performed to assess the expression of an adhesion molecule (B) ICAM1, and proliferation marker (C) Ki67. The images were captured by a bright field microscope at ×400 magnification and the figure shows representative images of staining.

elicited remarkable induction of antioxidant regulators SOD1 and Nrf-2 expression, thus counterbalanced the ROS by activating compensatory mechanisms, and concomitantly decreased the expression of NF-κB and nitrotyrosine. This observation was further strengthened with the results of immunoblot analysis. It is likely that the inhibition of MAPKs and NF-κB crosstalk by AMB might be due to the reduction of oxidative damage [51].

Topical application of IMQ induces skin inflammation by increasing myriad of inflammatory flux due to infiltration of immune cells and pronounced splenomegaly [52]. Consistent with the literature, we have found significant spleen enlargement after 6 days with IMQ application. We next sought to investigate the inflammation severity using PASI scoring. It has been found that mice of IMQ group showed prominent erythema, scale formation and accompanied by increased thickness in the dorsal region of the skin [28]. Furthermore, it was observed that AMB treatment prominently in topical route and moderately in SC route alleviated the splenomegaly and significantly decreased the erythema, scaling, skin fold and ear thickness as compared to IMQ group. AMB group showed similar changes comparatively with that of tacrolimus group. Based on the histopathological analysis, it was found that the epidermal layer of the skin in IMQ group was found to have elongated rete ridges protruding into dermis as a result of acanthosis in the skin. AMB topical treatment remarkably reduced the phenotypic changes associated with IMQ and decreased the vicinity of the affected skin.

The robust body of literature reported that, the IL-23/IL-17A cytokine axis is positively regulated in the pathogenesis of psoriasis [53], other cytokines including IL-1β, IL-6, IL-17A, IL-22, TGF-β, and TNF-α have been found to be elevated in lesional psoriasis skin and serum and this cluster of cytokines have been postulated to drive the psoriasis pathogenesis [54]. When assayed for the cytokines levels in skin tissues by ELISA, consistent with the previous reports, the significant increase in the production of IL-1β, IL-6, IL-17A, IL-22, TGF-β, and TNF-α have been found with IMQ application. Where, tacrolimus exhibited a considerable impact on T-cell response, by dampening the cytokine levels. Earlier it was found that AMB effectively reduced the IL-6, TNF-α, and TGF-β cytokines stimulated by LPS in bronchoalveolar lavage fluid of mice. In the present study, we found similar results with IMQ induction in the skin, apart from these cytokines IL-17A and IL-22 and IL-23 levels were found to be significantly reduced with AMB treatment. AMB exerted a stronger inhibitory effect on cytokine production mediated by T-cells and the effects are comparable with tacrolimus.

In conclusion, AMB treatment ameliorated the severity of IMQ induced psoriasis-like skin inflammation in mice, and its therapeutic effect is associated with downregulation of pro-inflammatory cytokines as

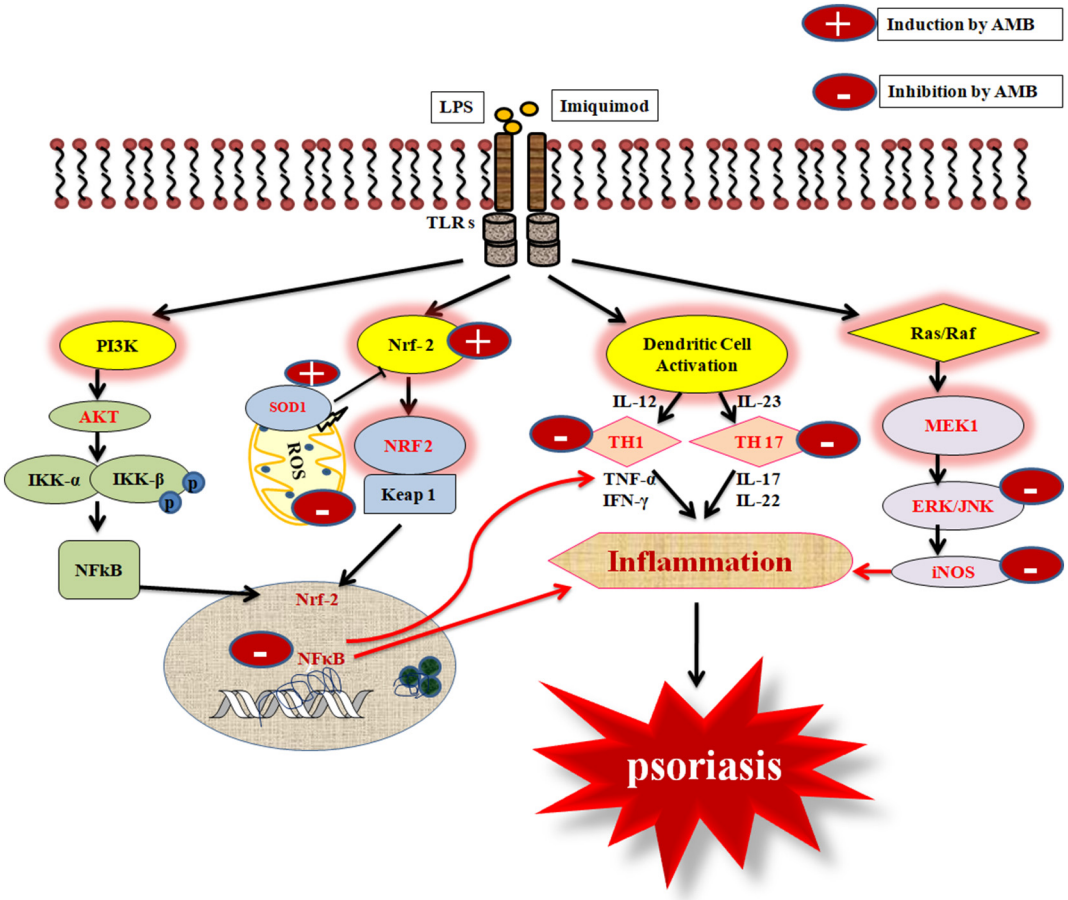

Fig. 8. AMB ameliorates the oxidative and nitrosative stress in psoriasis like skin inflammation. A schematic diagram represents the molecular mechanism and targets of AMB against LPS and IMQ induced inflammation.

well as regulating the oxidative/anti-oxidative redox equilibrium and hindering the inflammation associated signaling cascade (Fig. 8). As AMB treatment in humans is well tolerated with no major side effects, thus AMB treatment for psoriasis patients might offer an interesting cost-effective treatment option with negligible adverse effects.

Acknowledgements

Authors acknowledge to Department of Pharmaceuticals, Ministry of Chemicals and Fertilizers, Government of India and NIPER-Hyderabad for providing facilities for conducting the experiments. The authors would like to thank the Department of Biotechnology (DBT), Govt. of India for the financial support *via* North East-Twinning Grant: MAP/2015/58, Indo-Brazil Grant: DBT/IC-2/Indo-Brazil/2016-19/01 and DST-Science and Engineering Board-Early Career Research Award (SERB-ECR) Grant: ECR/2016/000007.

Conflict of interest

Authors declare no conflict of interest.

References

[1] X. Lin, T. Huang, Oxidative stress in psoriasis and potential therapeutic use of antioxidants, Free Radic. Res. 50 (2016) 585–595.
[2] D.P. Kadam, A.N. Suryakar, R.D. Ankush, C.Y. Kadam, K.H. Deshpande, Role of oxidative stress in various stages of psoriasis, Indian J. Clin. Biochem. 25 (2010) 388–392.
[3] N.K. Campbell, H.K. Fitzgerald, A. Malara, R. Hambly, C.M. Sweeney, B. Kirby, J.M. Fletcher, A. Dunne, Naturally derived Heme-Oxygenase 1 inducers attenuate inflammatory responses in human dendritic cells and T cells: relevance for psoriasis treatment, Sci. Rep. 8 (2018) 10287.
[4] A. Woźniak, G. Drewa, E. Krzyzyńska-Maliniowska, R. Czajkowski, F. Protas-Drozd, C. Mila-Kierzenkowska, M. Rozwodowska, M. Sopońska, E. Czarnecka-Zaba, Oxidant-antioxidant balance in patients with psoriasis, Med. Sci. Monit. Int. Med. J. Exp. Clin. Res. 13 (2007) CR30–33.
[5] S.R. Feldman, H. Tian, I. Gilloteau, P. Mollon, M. Shu, Economic burden of co-morbidities in psoriasis patients in the United States: results from a retrospective U.S. database, BMC Health Serv. Res. 17 (2017).
[6] R. Sruamsiri, K. Iwasaki, W. Tang, J. Mahlich, Persistence rates and medical costs of biological therapies for psoriasis treatment in Japan: a real-world data study using a claims database, BMC Dermatol. 18 (2018) 5.
[7] A.B. Janagond, P. Aparna, Biologicals in the treatment of psoriasis: the Indian perspective, BLDE Univ. J. Health Sci. (2017) 9–13.
[8] N. Malecic, H. Young, Tacrolimus for the management of psoriasis: clinical utility and place in therapy, Psoriasis Auckl. NZ. 6 (2016) 153–163.
[9] J. Castellsague, J.G. Kuiper, A. Pottegård, I. Anveden Berglind, D. Dedman, L. Gutierrez, B. Calingaert, M.P. van Herk-Sukel, J. Hallas, A. Sundström, A.M. Gallagher, J.A. Kaye, C. Pardo, K.J. Rothman, S. Perez-Gutthann, A cohort study on the risk of lymphoma and skin cancer in users of topical tacrolimus, pimecrolimus, and corticosteroids (Joint European Longitudinal Lymphoma and Skin Cancer Evaluation - JOELLE study), Clin. Epidemiol. 10 (2018) 299–310.
[10] M. Matoshvili, A. Katsitadze, T. Sanikidze, D. Tophuria, A. Richetta, S. D'Epiro, The role of nitric oxide in the pathogenesis and severity of psoriasis, Georgian Med. News (2014) 61–64.
[11] I. Haase, R.M. Hobbs, M.R. Romero, S. Broad, F.M. Watt, A role for mitogen-activated protein kinase activation by integrins in the pathogenesis of psoriasis, J. Clin. Invest. 108 (2001) 527–536.
[12] R.M. Andrés, M.C. Montesinos, P. Navalón, M. Payá, M.C. Terencio, NF-κB and STAT3 inhibition as a therapeutic strategy in psoriasis: in vitro and in vivo effects of BTH, J. Invest. Dermatol. 133 (2013) 2362–2371.
[13] M.J. Morgan, Z. Liu, Crosstalk of reactive oxygen species and NF-κB signaling, Cell Res. 21 (2011) 103–115.
[14] S. Yan, et al., NF-κB-induced microRNA-31 promotes epidermal hyperplasia by repressing protein phosphatase 6 in psoriasis, Nat. Commun. 3 (6) (2015) 7652.
[15] H. Takahashi, M. Ibe, S. Nakamura, A. Ishida-Yamamoto, Y. Hashimoto, H. Iizuka, Extracellular regulated kinase and c-Jun N-terminal kinase are activated in psoriatic involved epidermis, J. Dermatol. Sci. 30 (2002) 94–99.
[16] P.R. Gupta, Ambroxol - resurgence of an old molecule as an anti-inflammatory

agent in chronic obstructive airway diseases, Lung India Off. Organ Indian Chest Soc. 27 (2010) 46–48.
[17] D. Olivieri, G. Zavattini, G. Tomasini, S. Daniotti, G. Bonsignore, G. Ferrara, N. Carnimeo, R. Chianese, E. Catena, S. Marcatili, Ambroxol for the prevention of chronic bronchitis exacerbations: long-term multicenter trial. Protective effect of ambroxol against winter semester exacerbations: a double-blind study versus placebo, Respir. Int. Rev. Thorac. Dis. 51 (Suppl. 1) (1987) 42–51.
[18] M. Plomer, J. de Zeeuw, [More than expectorant: new scientific data on ambroxol in the context of the treatment of bronchopulmonary diseases], MMW Fortschr. Med. 159 (2017) 22–33.
[19] Q.M. Zhi, L.T. Yang, H. Sun, Protective effect of ambroxol against paraquat-induced pulmonary fibrosis in rats, Intern. Med. Tokyo Jpn. 50 (2011) 1879–1887.
[20] X. Su, L. Wang, Y. Song, C. Bai, Inhibition of inflammatory responses by ambroxol, a mucolytic agent, in a murine model of acute lung injury induced by lipopolysaccharide, Intensive Care Med. 30 (2004) 133–140.
[21] M. Malerba, B. Ragnoli, Ambroxol in the 21st century: pharmacological and clinical update, Expert Opin. Drug Metab. Toxicol. 4 (2008) 1119–1129.
[22] K. Nobata, M. Fujimura, Y. Ishiura, S. Myou, S. Nakao, Ambroxol for the prevention of acute upper respiratory disease, Clin. Exp. Med. 6 (2006) 79–83.
[23] G.H.B. Maegawa, M.B. Tropak, J.D. Buttner, B.A. Rigat, M. Fuller, D. Pandit, L. Tang, G.J. Kornhaber, Y. Hamuro, J.T.R. Clarke, D.J. Mahuran, Identification and characterization of ambroxol as an enzyme enhancement agent for Gaucher disease, J. Biol. Chem. 284 (2009) 23502–23516.
[24] P.R. Gupta, Ambroxol hydrochloride in the management of idiopathic pulmonary fibrosis: clinical trials are the need of the hour, Lung India Off. Organ Indian Chest Soc. 31 (2014) 43–46.
[25] R. Tokala, S. Thatikonda, S. Sana, P. Regur, C. Godugu, N. Shankaraiah, Synthesis and in vitro cytotoxicity evaluation of β-carboline-linked 2,4-thiazolidinedione hybrids: potential DNA intercalation and apoptosis-inducing studies, New J. Chem. 42 (2018) 16226–16236.
[26] L. Van der Fits, et al., Imiquimod-induced psoriasis-like skin inflammation in mice is mediated via the IL-23/IL-17 axis, J. Immunol. 182 (2009) 5836–5845.
[27] A. Jain, V. Pooladanda, U. Bulbake, S. Doppalapudi, T.A. Rafeeqi, C. Godugu, W. Khan, Liposphere mediated topical delivery of thymoquinone in the treatment of psoriasis, Nanomedicine Nanotechnol. Biol. Med. 13 (2017) 2251–2262.
[28] T.T. Di, Z.T. Ruan, J.X. Zhao, Y. Wang, X. Liu, Y. Wang, P. Li, Astilbin inhibits Th17 cell differentiation and ameliorates imiquimod-induced psoriasis-like skin lesions in BALB/c mice via Jak3/Stat3 signaling pathway, Int. Immunopharmacol. 32 (32) (2016) 38.
[29] N. Umasuthan, S.D.N.K. Bathige, K.S. Revathy, Y. Lee, I. Whang, C.Y. Choi, H.-C. Park, J. Lee, A manganese superoxide dismutase (MnSOD) from Ruditapes philippinarum: comparative structural- and expressional-analysis with copper/zinc superoxide dismutase (Cu/ZnSOD) and biochemical analysis of its antioxidant activities, Fish Shellfish Immunol 33 (2012) 753–765.
[30] S. Das, M. Kumar, V. Negi, B. Pattnaik, Y.S. Prakash, A. Agrawal, B. Ghosh, MicroRNA-326 regulates profibrotic functions of transforming growth factor-β in pulmonary fibrosis, Am. J. Respir. Cell Mol. Biol. 50 (2014) 882–892.
[31] J. Baliwag, D.H. Barnes, A. Johnston, Cytokines in psoriasis, Cytokine 73 (2015) 342–350.
[32] S. Bale, P. Venkatesh, M. Sunkoju, C. Godugu, An adaptogen: withaferin A ameliorates in vitro and in vivo pulmonary fibrosis by modulating the interplay of fibrotic, matricelluar proteins, and cytokines, Front. Pharmacol. 9 (2018).
[33] V. Pooladanda, S. Bandi, S.R. Mondi, K.M. Gottumukkala, C. Godugu, Nimbolide epigenetically regulates autophagy and apoptosis in breast cancer, Toxicol. Vitro Int. 51 (2018) 114–128.
[34] V. Pooladanda, S. Thatikonda, S. Bale, B. Pattnaik, D.K. Sigalapalli, N.B. Bathini, S.B. Singh, C. Godugu, Nimbolide protects against endotoxin-induced acute respiratory distress syndrome by inhibiting TNF-α mediated NF-κB and HDAC-3 nuclear translocation, Cell Death Dis. 10 (2019) 81.
[35] X. Ci, J. Zhou, H. Lv, Q. Yu, L. Peng, S. Hua, Betulin exhibits anti-inflammatory activity in LPS-stimulated macrophages and endotoxin-shocked mice through an AMPK/AKT/Nrf2-dependent mechanism, Cell Death Dis. 8 (2017) e2798.
[36] Y. Tan, Q. Qi, C. Lu, X. Niu, Y. Bai, C. Jiang, Y. Wang, Y. Zhou, A. Lu, C. Xiao, Cytokine imbalance as a common mechanism in both psoriasis and rheumatoid arthritis, Mediat. Inflamm. 2017 (2017) 1–13.
[37] S. Zhang, J. Jiang, Q. Ren, Y. Jia, J. Shen, H. Shen, X. Lin, H. Lu, Q. Xie, Ambroxol inhalation ameliorates LPS-induced airway inflammation and mucus secretion through the extracellular signal-regulated kinase 1/2 signaling pathway, Eur. J. Pharmacol. 775 (2016) 138–148.
[38] S. Kanie, M. Yokohira, K. Yamakawa, Y. Nakano-Narusawa, S. Yoshida, N. Hashimoto, K. Imaida, Suppressive effects of the expectorant drug ambroxol hydrochloride on quartz-induced lung inflammation in F344 rats, J. Toxicol. Pathol. 30 (2017) 153–159.
[39] A. Gillissen, D. Nowak, Characterization of N-acetylcysteine and ambroxol in antioxidant therapy, Respir. Med. 92 (4) (2018) 609–623.
[40] J. An, T. Li, Y. Dong, Z. Li, J. Huo, Terminalia chebulanin attenuates psoriatic skin lesion via regulation of heme oxygenase-1, Cell. Physiol. Biochem. 39 (2016) 531–543.
[41] P. Zanvit, W. Chen, Role of regulatory T cells and TGF-β in an experimental model of psoriasis in mice (71.8), J. Immunol. 188 (2012) 71.8.
[42] F. Aktan, iNOS-mediated nitric oxide production and its regulation, Life Sci. 75 (2004) 639–653.
[43] U. Forstermann, W.C. Sessa, Nitric oxide synthases: regulation and function, Eur. Heart J. 33 (2012) 829–837.
[44] C. Yang, L. You, X. Yin, Y. Liu, X. Leng, W. Wang, N. Sai, J. Ni, C. Yang, L. You, X. Yin, Y. Liu, X. Leng, W. Wang, N. Sai, J. Ni, Heterophyllin B ameliorates lipopolysaccharide-induced inflammation and oxidative stress in RAW 264.7 macrophages by suppressing the PI3K/Akt pathways, Molecules 23 (2018) 717.
[45] C. Choi, H. Cho, J. Park, C. Cho, Y. Song, Suppressive effects of genistein on oxidative stress and NFkappaB activation in RAW 264.7 macrophages, Biosci. Biotechnol. Biochem. 67 (2003) 1916–1922.
[46] M.A. Lowes, F. Chamian, M.V. Abello, J. Fuentes-Duculan, S.-L. Lin, R. Nussbaum, I. Novitskaya, H. Carbonaro, I. Cardinale, T. Kikuchi, P. Gilleaudeau, M. Sullivan-Whalen, K.M. Wittkowski, K. Papp, M. Garovoy, W. Dummer, R.M. Steinman, J.G. Krueger, Increase in TNF-α and inducible nitric oxide synthase-expressing dendritic cells in psoriasis and reduction with efalizumab (anti-CD11a), Proc. Natl. Acad. Sci. 102 (2005) 19057–19062.
[47] J.O. Baek, D. Byamba, W.H. Wu, T.G. Kim, M.-G. Lee, Assessment of an imiquimod-induced psoriatic mouse model in relation to oxidative stress, Arch. Dermatol. Res. 304 (2012) 699–706.
[48] C. Johansen, A.T. Funding, K. Otkjaer, K. Kragballe, U.B. Jensen, M. Madsen, L. Binderup, T. Skak-Nielsen, M.S. Fjording, L. Iversen, Protein expression of TNF-alpha in psoriatic skin is regulated at a posttranscriptional level by MAPK-activated protein kinase 2, J. Immunol. Baltim. Md 176 (2006) (1950) 1431–1438.
[49] A.M. Goldminz, S.C. Au, N. Kim, A.B. Gottlieb, P.F. Lizzul, NF-κB: an essential transcription factor in psoriasis, J. Dermatol. Sci. 69 (2013) 89–94.
[50] M.Y. Peroval, A.C. Boyd, J.R. Young, A.L. Smith, A critical role for MAPK signalling pathways in the transcriptional regulation of toll like receptors, PLoS One 8 (2013) e51243.
[51] E. Bognar, Z. Sarszegi, A. Szabo, B. Debreceni, N. Kalman, Z. Tucsek, B. Sumegi, F.G. Jr, Antioxidant and anti-inflammatory effects in RAW264.7 macrophages of malvidin, a major red wine polyphenol, PLoS One 8 (2013) e65355.
[52] P. Redondo, J. del Olmo, A. López-Diaz de Cerio, S. Inoges, M. Marquina, I. Melero, M. Bendandi, Imiquimod enhances the systemic immunity attained by local cryosurgery destruction of melanoma lesions, J. Invest. Dermatol. 127 (2007) 1673–1680.
[53] Y.J. Jeon, S.K. Sah, H.S. Yang, J.H. Lee, J. Shin, T.Y. Kim, Rhododendrin inhibits toll-like receptor-7-mediated psoriasis-like skin inflammation in mice, Exp. Mol. Med. 49 (2017) e349.
[54] J. Sun, Y. Zhao, J. Hu, Curcumin inhibits imiquimod-induced psoriasis-like inflammation by inhibiting IL-1beta and IL-6 production in mice, PLoS One 8 (2013) e67078.